TISSUE ENGINEERING: Part A
Volume 19, Numbers 3 and 4, 2013

DOI: 10.1089/ten.tea.2012.0052

Porosity and Cell Preseeding Influence Electrospun Scaffold Maturation and Meniscus Integration *In Vitro*

Lara C. Ionescu, PhD, and Robert L. Mauck, PhD

Electrospinning generates fibrous scaffolds ideal for engineering soft orthopedic tissues. By modifying the electrospinning process, scaffolds with different structural organization and content can be generated. For example, fibers can be aligned in a single direction, or the porosity of the scaffold can be modified through the use of multi-jet electrospinning and the removal of sacrificial fibers. In this work, we investigated the role of fiber alignment and scaffold porosity on construct maturation and integration within *in vitro* meniscus defects. Further, we explored the effect of preseeding expanded meniscus fibrochondrocytes (MFCs) onto the scaffold at a high density before *in vitro* repair. Our results demonstrate that highly porous electropun scaffolds integrate better with a native tissue and mature to a greater extent than low-porosity scaffolds, while scaffold alignment does not influence integration or maturation. The addition of expanded MFCs to scaffolds before *in vitro* repair improved integration with the native tissue, but did not influence maturation. In contrast, preculture of these same scaffolds for 1 month before repair decreased integration with the native tissue, but resulted in a more mature scaffold compared to implantation of cellular scaffolds or acellular scaffolds. This work will inform scaffold selection in future *in vivo* studies by identifying the ideal scaffold and seeding methods for meniscus tissue engineering.

Introduction

Interest in electrospun scaffolds for fibrous tissue engineering has grown dramatically in recent years. These scaffolds have been used in a wide range of applications, including cardiovascular, skin, neurological, and orthopedic tissue engineering.[1–9] The ability to electrospin a wide range of materials, including synthetic and natural polymers, the potential to include drug delivery, and the ease of tuning fiber properties, provide a wide array of scaffolds to explore for defined clinical applications.[2] Importantly, electrospun scaffolds can mimic both the structural and mechanical anisotropy of fibrous tissues as well as withstand the high loads that are imposed on the tissues during physiologic motion.[1] Depending on the choice of material, cells will attach, proliferate, and deposit matrix in these structures, improving the mechanical properties of the scaffolds over time.[2] For example, disc[8] meniscus,[7,9] as well as bovine and human mesenchymal stem cells[7–11] cells seeded on aligned and disorganized poly(ε-caprolactone) (PCL) scaffolds produced similar amounts of matrix, but the mechanical properties of aligned scaffolds were 7-times higher than disorganized scaffolds, approaching that of the native meniscus,[7] after just 10 weeks of *in vitro* culture. These findings indicate that scaffold architecture can dictate long-term maturation, where maturation refers to increases in cell density and distribution, as well as an ordered accumulation of collagen and proteoglycan that is directly related to improvements in mechanical properties.

One drawback of electrospun materials is that the structure is quite dense, which can limit cell infiltration into the scaffold.[9] Uneven distribution of cells prevents the development of homogeneous matrix, and so limits improvements in mechanical properties. To promote cell infiltration and matrix production, we and others have explored a number of different techniques. One approach is to construct multilamellar constructs seeded layer by layer[12] and to supplement with growth factors that specifically enhance activity of native cell types.[13] Alternatively, one can modify the culture conditions; culturing cell seeded nanofibrous materials in a hydrodynamic environment after seeding results in better cell infiltration, although the technique limits matrix accumulation over time.[14] Alternatively, multi-jet electrospinning can be used to create scaffolds with distinct fiber populations that degrade at different rates.[15,16] For instance, slow-degrading PCL fibers can be intermingled with water soluble poly(ethylene oxide) (PEO) fibers. Upon hydration, these sacrificial PEO fibers dissolve, leaving a more porous architecture of aligned PCL fibers. Scaffolds of varying porosities can be fabricated by changing the relative percentage of sacrificial PEO fibers to PCL fibers. Previously, we found that increased porosity resulted in better cell infiltration and matrix distribution, although there was an associated

McKay Orthopaedic Research Laboratory, Department of Orthopaedic Surgery, Perelman School of Medicine, University of Pennsylvania, Philadelphia, Pennsylvania.

decrease in mechanical strength and dimensional stability at very high sacrificial levels.[15]

While cell-seeded electropun scaffolds will mature *in vitro*, and this can be expedited by increasing sacrificial fiber content, another equally important consideration is how such materials integrate with the native meniscus tissue. If electrospun scaffolds are to replace regions of resected tissue (a common procedure called meniscectomy, the most prevalent orthopedic surgery in the U.S.[17]), their initial and long-term integration with native structures is of paramount importance. Previously, we utilized an *in vitro* explant defect model to assess the integration potential of the native tissue as a function of age.[18] In this system, the force required to separate apposing pieces of tissue arranged as concentric cylinders (i.e., the integration strength) was determined. This approach has been used in both meniscus and cartilage tissue engineering to assess tissue–tissue and tissue–biomaterial integration.[19–22] In our prior study, we also replaced the inner core of the meniscus defect with a disc of electrospun scaffold, and found that native meniscus cells migrated into the material after 6 weeks of *in vitro* culture. Here, we expand upon this model to test the mechanical integration strength between the native tissue and electrospun scaffolds of varying composition and organization. We hypothesized that increasing scaffold porosity would improve both the maturation and integration strength of the scaffolds *in vitro*, where integration strength refers to the force required to separate the scaffold from the meniscus explant after time in culture.

An additional consideration is whether scaffolds should be seeded before implantation. Clinically, implantation of acellular materials into a meniscal defect is the simplest and most cost effective approach for repair. As noted above, prior studies have demonstrated that nanofibrous materials are readily populated by native meniscus cells *in vitro*. Indeed, other acellular scaffolds, such as the collagen meniscus implant,[23] have been implanted adjacent to the meniscus and became colonized by endogenous cells. However, acellular electrospun scaffolds are delicate, and are particularly susceptible to compaction upon exposure to compressive forces. Thus, postoperative rehabilitation will require a significant period of non-weight bearing, which can be challenging for the patient. As the scaffold becomes colonized by local cells and the matrix is deposited, the new extracellular matrix will reinforce the nanofibrous architecture in compression.[24] One approach to reduce the non-weight bearing period would be to implant mature scaffolds already colonized by cells. Preseeded or precultured scaffolds might also integrate more rapidly with the native tissue given the increase in early cell number at the construct border. To address this issue, we evaluated the effect of the direct addition of expanded meniscus fibrochondrocytes (MFCs) to the scaffold immediately before *in vitro* defect repair, as well as placement after a 1-month preculture period. We hypothesized that both such steps would improve integration, with precultured scaffolds exhibiting the most robust maturation and integration.

Materials and Methods

Fabrication of electrospun scaffolds with varying alignment and porosity

To create electrospun scaffolds, two separate solutions (14.3% w/v poly(ε-caprolactone) (PCL, 80 kDa; Sigma-Aldrich, St. Louis, MO) in a 1:1 mixture of tetrahydrofuran (THF, Fisher Chemical, Fairlawn, NJ) and N,N-dimethylformamide (DMF; Fisher Chemical) and 10% polyethylene oxide (PEO, 200 kDa; Polysciences, Warrington, PA) in 90% EtOH)[15] were mixed overnight before electrospinning. Two fabrication methods were used to alter the fiber organization in pure PCL scaffolds (disorganized and aligned) and three levels of PEO fiber fraction (0%, 30%, 60%) inclusion were used to vary the porosity of aligned scaffolds, creating four distinct scaffold formulations for analysis (Fig. 1A). To create disorganized PCL scaffolds, a 20-mL syringe was filled with the PCL electrospinning solution and fitted with a stainless steel 18G blunt-ended needle that served as a charged spinneret. A flow rate of 2.5 mL/h was maintained with a syringe pump (KDS100; KD Scientific, Holliston, MA). A power supply (ES30N-5W; Gamma High Voltage Research, Inc., Ormond Beach, FL) applied a +13 kV potential difference between the spinneret and the grounded mandrel located at a distance of 12 cm from the spinneret. Additionally, two aluminum shields charged to +10 kV were placed perpendicular to and on either side of the mandrel to better direct the electrospun fibers toward the grounded mandrel. The mandrel was slowly rotated via a belt mechanism conjoined to an AC motor (Pacesetter 34R; Bodine Electric, Chicago, IL) at a speed of 0.34 m/s to cover the collecting surface while limiting alignment.

To fabricate the remaining three aligned scaffolds, a custom trijet electrospinning device[16] was utilized to generate an intermingled composite of PCL and PEO fibers. Three syringes were fitted with needles, as described previously, and were directed at a single central rotating mandrel (surface velocity of 10 m/s) equidistant from each other and separated by shields (+5 kV charge). The speed of the mandrel was sufficiently fast to align the collected fibers in a single direction. A flow rate of 2 mL/h and a +15 potential difference between the needles and mandrel was utilized. The distance between the mandrel and the needle was 12 cm. The needles followed a reciprocating path using a custom fanner to disperse the fibers along the length of the mandrel. As depicted in Figure 1A, the following configurations were used to create each of the three aligned scaffolds: 3 jets of PCL to create Low-Porosity, 1 jet of PCL/1 jet of PEO to create Medium-Porosity, and 1 jet of PCL/2 jets of PEO to create High-Porosity scaffolds. The resulting PCL content was 100%, 70%, and 30%, respectively. The grading (low, medium, high) indicates the relative porosity of the material after PEO removal. A total volume of 20 mL of spinning solution was used to generate each mat with a final thickness of ~1 mm before PEO removal. After fabrication, 4-mm discs were excised using a dermal punch and stored in a dessicator until use. The percent of PEO incorporation was verified by measurement of mass loss following exposure to an aqueous solution. Scaffolds were routinely imaged by scanning electron microscopy (SEM) as in our previous studies, both before and after PEO removal.[15]

Formation of meniscus/scaffold constructs

Menisci were dissected from the knee joints of juvenile (3 months old) bovine limbs in a sterile manner. The bovine tissue was acquired from a slaughterhouse and is considered a by-product tissue under regulations of the animal care and use committee at the University of Pennsylvania. Cylinders (8 mm diameter ×3 mm thick) were excised centrally in the

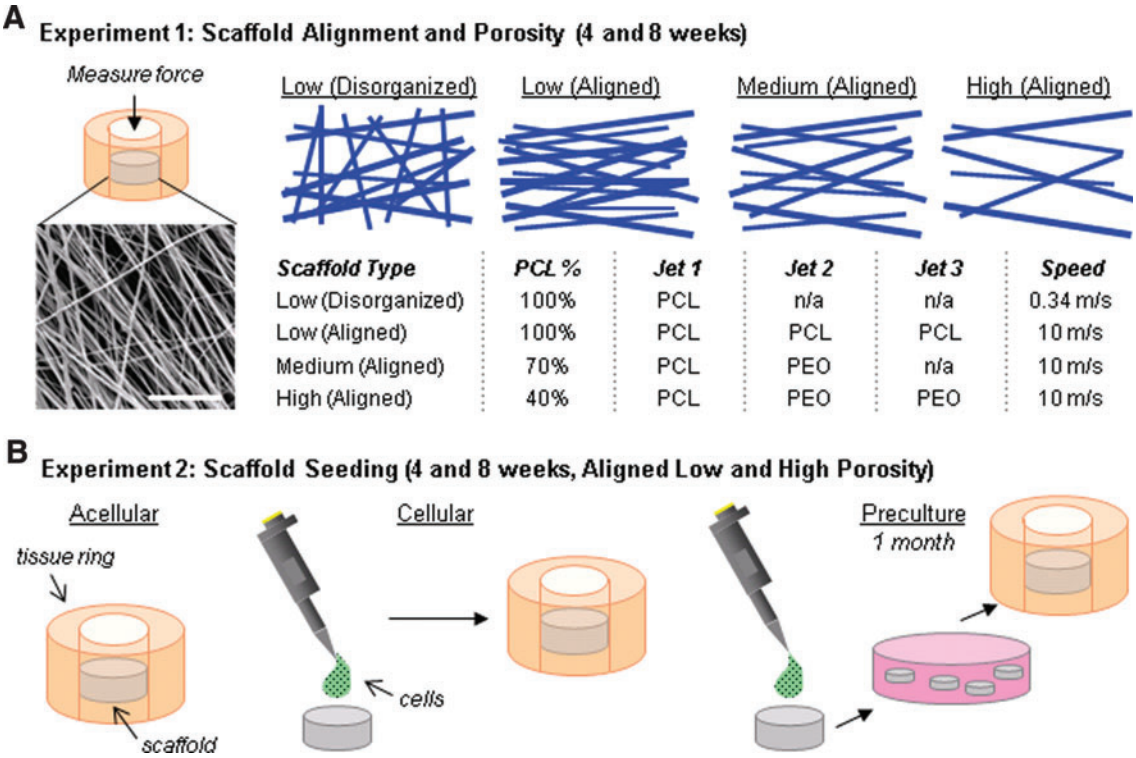

FIG. 1. Schematic illustration of study design. **(A)** Electrospun scaffolds with varying organization and porosity (fabrication details described in table) were implanted into cylindrical defects in meniscus explants. After *in vitro* culture, integration strength of the biomaterial with native tissue was determined (scale = 20 μm). **(B)** Three seeding techniques were evaluated: acellular (no cells added; scaffold populated directly from tissue), cellular (addition of cells before implantation), and preculture (cells added and seeded constructs precultured for 1 month before implantation). PCL, poly(ε-caprolactone). Color images available online at www.liebertpub.com/tea

axial direction using a dermal punch (Miltex, Plainsboro, NJ). A smaller dermal punch (4 mm diameter) was used to remove a central core from the cylinder to form a ring, and an electrospun disc was press-fit into the meniscus ring as depicted in Figure 1A.[18] Before insertion, scaffolds were exposed to the UV light for 10 min per side.

Production of scaffolds with different alignment and porosity

Electrospinning was carried out as described above to generate disorganized low-porosity, aligned low-porosity, aligned medium-porosity, and aligned high-porosity scaffolds ($n = 7$–9/condition, all work performed in duplicate, one representative data set shown). To determine if the presence of the meniscus tissue influenced scaffold maturation, tissue-free control scaffolds were cultured by seeding MFCs directly onto both sides of the four types of scaffold discs at a density of 3333 MFCs/mm^2 scaffold per side ($n = 6$–7/condition, work performed in duplicate, one representative data set shown). MFCs were isolated using sterile techniques from a 5-mm radial slice of juvenile meniscus by mincing the tissue into 2-mm^3 pieces and allowing the cells to migrate out onto the tissue culture plastic (Corning, Sigma-Aldrich, St. Louis, MO) to establish primary cultures over the course of 2 weeks. For expansion, cells were cultured in basal media [Dulbecco's modified Eagle's medium (DMEM) with 10% fetal bovine serum (FBS) and 1% penicillin/streptomycin/fungizone (PSF)]. After formation, the tissue-free control scaffolds and scaffold/meniscus repair constructs were cultured in DMEM with 10% FBS, 1% PSF, 50 μg/mL ascorbate-2-phosphate (vitamin C), and 10 ng/mL TGF-β3. After 4 and 8 weeks, samples were removed from culture and prepared for histology (control scaffolds and repair constructs) or tested mechanically (repair constructs only).

Mechanical integration strength between the scaffold and the native meniscus tissue was measured using a custom push-through testing device.[18] Briefly, an Instron 5848 was outfitted with a 3.5-mm-diameter indenter in series with a 50-N-load cell. This indenter was placed above a plate with a 5-mm-diameter hole. The construct was placed onto the plate, and the indenter progressed through the defect site at a rate of 0.0833 mm/s. Integration strength was calculated using the following formula:

$$Integration\ Strength = \frac{Maximum\ force(N)}{2\pi r \cdot h}$$

The height (h) of the scaffold disc was measured using an OptoNCDT laser measuring device (Micro-Epsilon, Raleigh, NC) after pushout.

After testing, the native tissue was discarded and the scaffold was lyophilized and digested in a buffer containing 2% papain at 60°C. The resulting digest was used to assess the DNA content (PicoGreen Assay; Invitrogen, Carlsbad, CA) and the glycosaminoglycan (GAG) content (dimethylmethylene blue (DMMB) assay[25]). Results were normalized to sample dry weight. To assess cell and matrix distribution, 1–2 fresh constructs per condition were prepared for histology by

fixing the samples in 4% paraformaldahyde overnight, embedding in optimal cutting temperature (OCT) freezing media (Tissue-Tek, Fisher, Fairlawn, NJ) and cryosectioning onto glass slides (12 μm thick) perpendicular to the plane of the electrospun disc. Slides were stained with Alcian blue for proteoglycans, Picrosirius red for collagen, and DAPI (Prolong Gold, Invitrogen, Carlsbad, CA) to identify cell nuclei.[18]

Production of cell-seeded scaffolds

To assess the role of cell seeding (Fig. 1B) on maturation and integration, juvenile bovine MFCs were seeded onto aligned low- and high-porosity scaffolds as previously described. Scaffold discs were seeded and immediately implanted (Cellular), or seeded and cultured for 4 weeks before implantation (Preculture). Acellular scaffolds were also inserted as a control (Acellular) ($n = 7$–8/group, performed in duplicate, one representative data set shown). After 4 and 8 weeks, constructs were processed for histology and mechanical integration as previously described.

Statistical analysis

For all work, 1- and 2-way ANOVAs were performed using SYSTAT software (Chicago, IL) to establish significant differences as a function of time, scaffold formulation, and/or seeding condition, followed by Tukey's *post hoc* testing to enable pairwise comparisons between groups. Significance was set at $p \leq 0.05$.

Results

Impact of scaffold architecture (alignment and porosity) on maturation and integration

Four types of electrospun scaffolds were created with various alignments and porosities. The disorganized scaffold had no prevailing fiber direction, whereas the aligned scaffolds had a single predominant fiber direction (Fig. 2A). SEM analysis revealed greater apparent porosity in high PEO content aligned scaffolds, compared to low and medium PEO content scaffolds, which did not differ markedly from one another. When scaffolds were seeded with expanded MFCs and cultured for 8 weeks, histology revealed the formation of cell- and matrix-dense envelopes around the scaffolds, which we refer to as a "capsule." While no differences were observed histologically between disorganized and aligned scaffolds, higher porosity scaffolds were better infiltrated (Fig. 2B) and had a more uniform matrix deposition of proteoglycan and collagen (Fig. 2C). Increasing porosity resulted in incrementally higher levels of DNA and GAG in the scaffold ($p < 0.05$) (Fig. 2D).

To test the impact of scaffold architecture and porosity on cell colonization directly from the native tissue, we inserted discs of four different formulations of the acellular scaffold (as outlined in Fig. 1A) into circular meniscus defects and evaluated infiltration into the scaffold and mechanical integration with the native tissue. This approach mimics the implantation of an acellular scaffold *in vivo*. High-porosity aligned scaffolds integrated with the native tissue to a much greater degree than low-porosity aligned scaffolds, with a threefold improvement in integration strength at 8 weeks ($p < 0.05$) (Fig. 3A). Fiber alignment did not modulate the integration capacity for the low-porosity scaffolds, though this will be important in *in vivo* applications where collagen fiber continuity is essential to efficient load bearing in tension. Scaffolds pushed out of meniscus rings were digested and the biochemical content measured after 8 weeks *in vitro*. Quantification confirmed that twice as many cells (as determined by DNA content) per weight of scaffold populated high-porosity scaffolds compared to low-porosity scaffolds ($p < 0.05$) (Fig. 3B). Further, scaffold porosity strongly

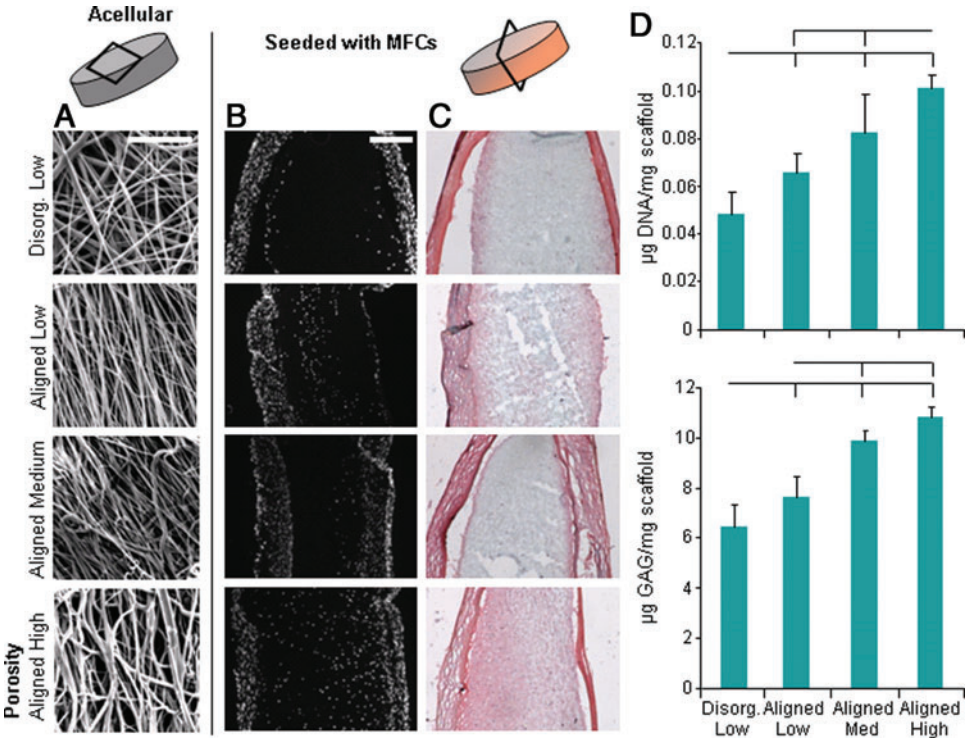

FIG. 2. Tissue-free control scaffolds seeded with culture expanded meniscus cells. **(A)** Scanning electron microscopy images of scaffold fiber morphology (scale = 20 μm). Cross section of scaffolds with **(B)** DAPI staining for cell nuclei and **(C)** Picrosirius red/Alcian blue staining for collagen/proteoglycan deposition (scale = 200 μm). **(D)** Quantification of DNA (top) and glycosaminoglycan (GAG) (bottom) content. Bars above indicate significant difference between groups (where the lack of vertical bar indicates origin for comparison to other groups), with $p < 0.05$; $n = 6$–7/condition. Color images available online at www.liebertpub.com/tea

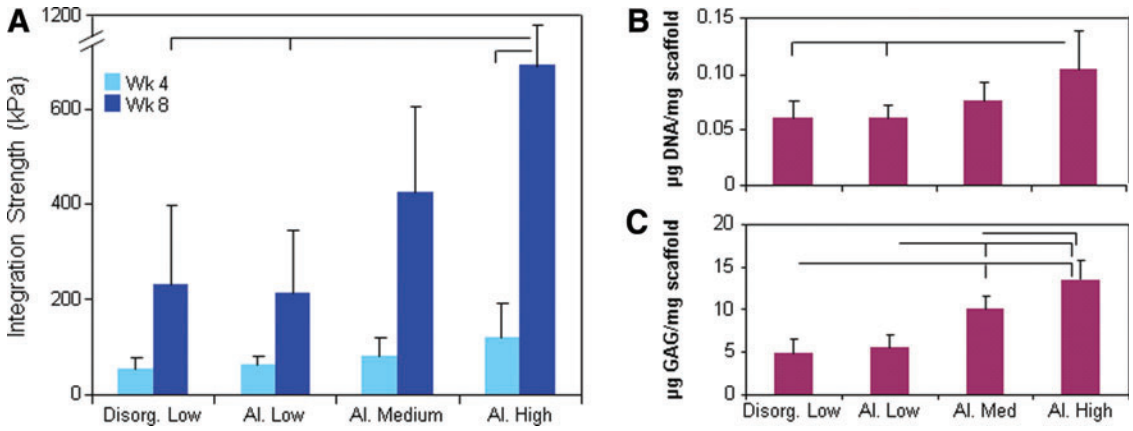

FIG. 3. Effect of scaffold architecture: Mechanical properties and biochemistry. **(A)** Integration strength between scaffold and native tissue with time in culture. DNA **(B)** and GAG **(C)** of scaffold after 8 weeks. Bars above indicate significant difference between groups (where the lack of vertical bar indicates origin for comparison to other groups), with $p < 0.05$; $n = 7$–8/condition. Color images available online at www.liebertpub.com/tea

influenced the GAG content, with low-, medium-, and high-porosity scaffolds containing incrementally more GAG after 8 weeks (Fig. 3C).

Histology showed that thin capsules comprised of cells and matrix formed around all scaffolds in this *in vitro* defect model; these capsules were less pronounced than in tissue-free control scaffolds (Fig. 4A, B). A new ancillary tissue was deposited between the scaffold and native tissue, creating a bridge of collagen and proteoglycan that influenced integration properties (Fig. 4A). The ancillary tissue was more pronounced in high-porosity scaffolds (*high-porosity scaffold shown in* Fig. 4A, *DAPI images of all groups in* Fig. 4B). Furthermore, high-porosity scaffolds showed the greatest cell distribution, with a similar cell density to the native meniscus tissue after 8 weeks in culture and an almost uniform cell distribution throughout the material (Fig. 4B, lower-right).

Impact of scaffold seeding and preculture on maturation and integration

Aligned low- and high-porosity scaffolds were next used to determine whether the seeding method influenced scaffold maturation and integration. While low-porosity scaffolds are the easiest to fabricate and are most extensively tested, high-porosity scaffolds demonstrated superior integration and maturation properties. Three different scaffold/meniscus repair constructs were formulated: acellular implantation, the addition of expanded MFCs immediately before insertion (cellular), and 4 weeks of preculture of seeded scaffolds before insertion (preculture). Mechanical testing revealed that, as previously shown, high-porosity acellular scaffolds integrated to a greater extent than low-porosity scaffolds after 8 weeks *in vitro* ($p < 0.05$) (Fig. 5A). Seeding the scaffold immediately before implantation with a high density of expanded MFCs resulted in significantly better integration in low-porosity scaffolds, but did not further improve high-porosity scaffold integration capacity compared to acellular constructs. Preculturing scaffolds for 4 weeks before implantation resulted in significantly lower integration strength for both scaffold types compared to cellular conditions ($p < 0.05$).

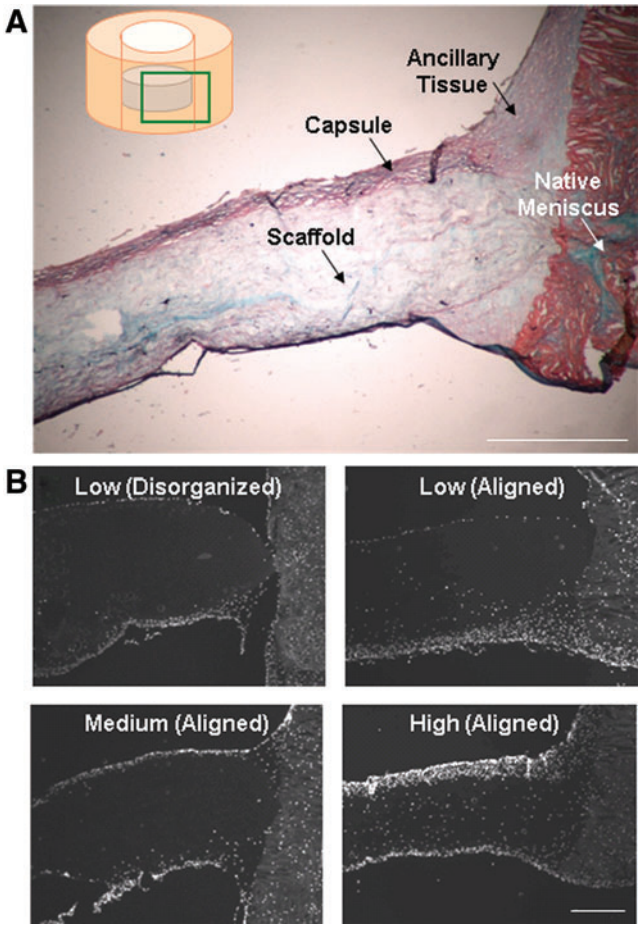

FIG. 4. Effect of scaffold architecture: Histology. **(A)** Alcian blue and Picrosirius red staining of high-porosity scaffold disc in meniscus defect for 8 weeks *in vitro* (scale = 500 µm). **(B)** DAPI staining of cell distribution through the scaffold at 8 weeks (scale = 500 µm). Color images available online at www.liebertpub.com/tea

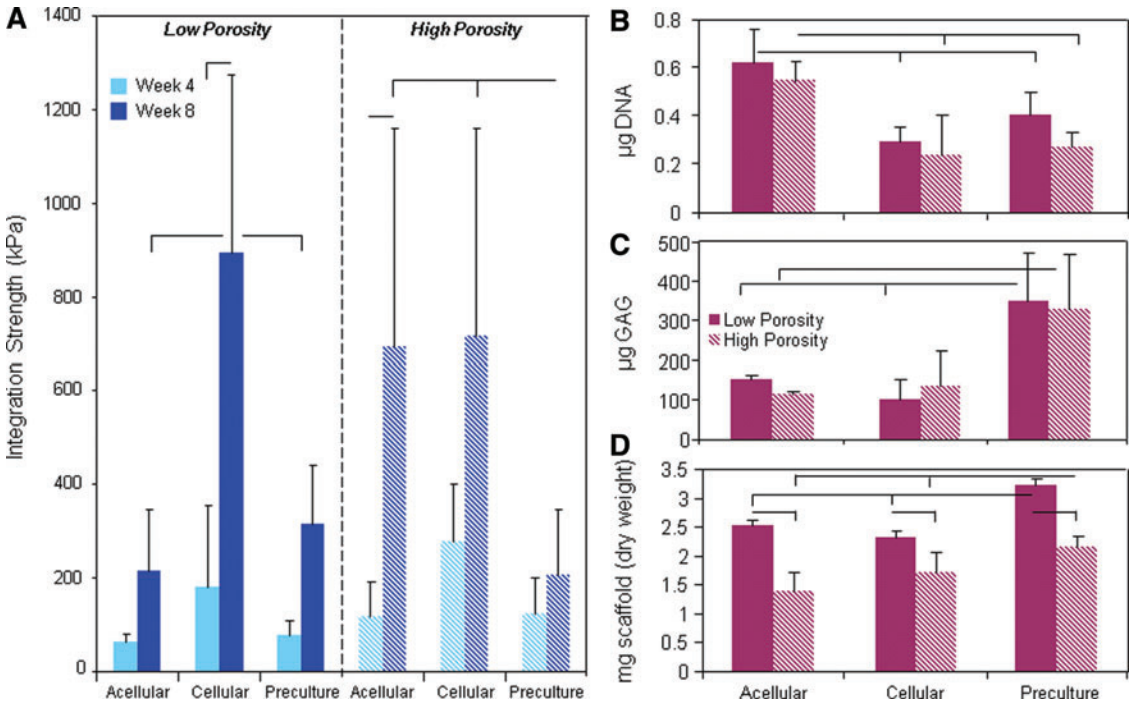

FIG. 5. Effect of cell seeding: Mechanical properties and biochemistry. **(A)** Integration strength of acellular, cellular, and precultured low- and high-porosity aligned scaffolds in a meniscus defect with time in culture. DNA **(B)** and GAG **(C)** content and dry weight **(D)** of scaffolds at 8 weeks as a function of scaffold porosity and seeding condition. Bars above indicate significant difference between groups (where the lack of vertical bar indicates origin for comparison to other groups), with $p < 0.05$; $n = 7–8$/condition. Color images available online at www.liebertpub.com/tea

Biochemical analysis of scaffolds revealed variable maturation based upon the seeding technique. Seeding expanded MFCs onto the scaffold (cellular and preculture conditions) resulted in lower cell densities in the scaffolds after 8 weeks compared to acellular controls, where MFCs populated the scaffold directly from the tissue (Fig. 5B). One extra month of preculture did not bolster the DNA content; however, it greatly increased the GAG content in the scaffold, suggesting that the cells were steadily accumulating matrix in the scaffold, with little proliferation, during the preculture period (Fig. 5C).

Histologically, cellular and preculture constructs had incrementally thicker cell capsules surrounding the scaffold compared to acellular controls (Fig. 6B). Examination of the scaffold/meniscus interface showed that the capsule in precultured samples appeared to prevent integration with the native tissue in preculture constructs. In contrast, cellular scaffolds had a tight connection with the native tissue (Fig. 6C, arrows).

Discussion

Dense connective tissues, such as the knee meniscus, suffer from low intrinsic repair capacity, low cell metabolic activity and density, and experience high mechanical stresses *in vivo* that are transmitted through their organized collagenous architecture. As such, advanced materials must be considered for engineering replacements that can successfully promote repair and re-establish complex joint mechanics.[9,12,15,26–28] One critical parameter for achieving such a goal for any material formulation will be its ability to integrate with native tissue structures. In this work, we employed a concentric explant model wherein a disc of electrospun scaffold was cultured inside an annulus of the native meniscus. Using this approach, we assessed both maturation (the histological and biochemical content of the implanted scaffold after 8 weeks) and integration of the scaffold to the native tissue (mechanical integration strength after 4 and 8 weeks) as a function of nanofiber alignment, scaffold porosity, and seeding technique.

Our results showed that scaffold alignment, while useful for directing new tissue formation,[7] did not on its own influence construct maturation or early integration strength in the meniscus defect. Fiber organization did not influence collagen/proteoglycan deposition or cell migration into or proliferation within scaffolds placed in *in vitro* meniscus defects. Moreover, fiber organization did not modulate matrix deposition at the meniscus/scaffold junction and so did not appreciably change integration strength. The alignment of the fibers in the scaffold with respect to the alignment of the collagen fibers in the tissue also did not appear to influence integration strength (*data not shown*). In the native meniscus, however, circumferentially directed hoop stresses transit through the organized collagen architecture. When this organization is lost (for example, in a disorganized, scarred repair of a radial tear), tensile properties are considerably lower and failures occur at the repair interface.[29] While the push-out test employed in this study did not identify differences in integration strength as a function of scaffold organization and alignment with respect to the native collagen bundle alignment, this organized connectivity could influence tensile load transmission under more physiologic testing scenarios (e.g., uniaxial tension) that engage these collagen fibers, and will be important for *in vivo* operation.

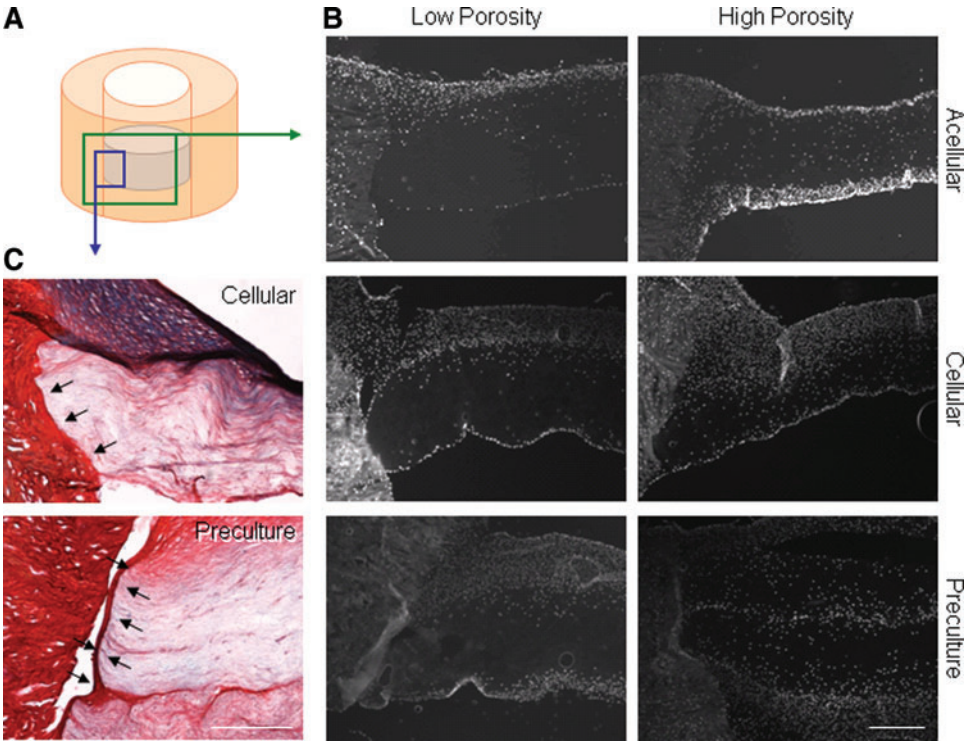

FIG. 6. Effect of cell seeding: Histology. **(A)** Schematic of histology sectioning planes. **(B)** DAPI staining to identify cell nuclei (scale = 500 μm). **(C)** Alcian blue and Picrosirius red staining of scaffold/meniscus construct. Arrow indicates junction between scaffold and meniscus tissue (high-porosity scaffold shown, scale = 250 μm). Color images available online at www.liebertpub.com/tea

While alignment had no effect on the integration capacity, the porosity of the implanted scaffold had a marked effect. In particular, we found that higher porosity nanofibrous scaffolds matured and integrated with the native tissue to a greater extent compared to their less porous counterparts. This is consistent with our previous data showing that cell infiltration is expedited with increasing sacrificial fiber content[15] as well as with other meniscus repair materials, where enhanced cellular infiltration and mechanical interlocking occurred when the native tissue was apposed to a more porous biomaterial surface compared to one with fewer and/or smaller pores.[30–33] For example, Pabbruwe *et al.* reported increased *in vitro* integration strength when using a collagen-based scaffold when the more porous surface of the material was apposed to the meniscus.[31] Similarly, in *in vivo* studies, a larger pore size in a polyurethane foam led to more rapid cellular colonization from the native meniscus.[32,33] Together with our current findings, these data suggest that the biomaterial should present a surface with increased porosity so as to expedite cellular colonization and mechanical interlocking with the native tissue. This is particularly true if scaffolds are to be implanted in an acellular form.

In an ideal scenario, an acellular meniscus implant would be implanted into a defect site, undergo rapid infiltration by native tissue cells, and mature *in situ* into a functional tissue over a short postoperative period. However, fibrous tissues, especially in the adult, have a low endogenous cellular content, and these cells may be constrained from migrating to the wound interface by the dense extracellular matrix in which they reside.[18] To address this issue, the biomaterial scaffold might be either preseeded with cells immediately before implantation, or matured *in vitro* until reaching functional equivalence with the native tissue. In this study, preseeding of meniscus cells onto the scaffold before placement in the defect markedly improved integration strength for the low-porosity aligned scaffolds (which showed poor integration when implanted in an acellular format). Addition of cells to high-porosity aligned scaffolds before placement in the defect did not alter the already robust integration capacity of that scaffold formulation. These findings suggest that cells at the interface play a significant role in both early and later mechanical interlocking between the native tissue and the implant, and that increasing their number at the implant periphery (either through direct seeding or increasing porosity) can improve the rate of mechanical stabilization of the wound interface. This finding is supported by the work of Peretti *et al.*, who showed that delivery of chondrocytes on devitalized meniscus pieces in a porcine meniscus defect model increased the repair capacity.[34] Similarly, Pabbruwe *et al.* showed that addition of mesenchymal stem cells to a collagen-based material increased integration strength *in vitro* compared to cell-free controls.[31] Likewise, Angele and coworkers showed that cellularization of a hyaluronan-based construct with stem cells, along with a short (2 week) preculture period, improved tissue formation and integration in a rabbit meniscus repair model.[35]

Interestingly, in our study, while immediate preseeding had a positive effect on integration, longer term preculture of scaffolds (1 month) limited integration. These constructs had the highest proteoglycan/collagen content and cellularity, but integration with the native tissue was markedly reduced. This finding might be related to the dense tissue rim observed on these precultured constructs, which could have impeded cellular interactions across the interface. Shorter culture periods, or removal of this dense boundary (through excision or digestion), might improve integration while still allowing for the implantation of a more mature construct.

While the results described above demonstrate the promise of a cellularized, highly porous, aligned nanofibrous scaffold for meniscus repair, there remain additional considerations that should be addressed as this technology moves toward *in vivo*, clinical translation. For example, while the concentric explant model has been used extensively to assess integration,[20,36,37] it does not test the most physiologically relevant forces experienced by the meniscus or the clinical scenario of replacement. Implanted engineered meniscus scaffolds will be exposed to simultaneous compressive forces and tensile forces, rather than the shear forces that arise in the push-out testing modality. However, the technique does provide information on the relative integration potential between scaffold types, which can motivate additional studies. While bioreactors and subcutaneous studies can mimic the *in situ* environment of the knee, direct implantation of the material into a meniscus defect will provide definitive evaluation of repair potential. Indeed, preliminary data from our group in a recently completed ovine meniscus implantation study suggests that these high-porosity constructs integrate better than their low-porosity counterparts after 12 weeks *in vivo*.[38] Translation of such findings to clinical relevance will necessitate the formation of implanted materials that can replace the greater part of the meniscus, rather than simply circular defects, to make up for the volumetric loss that occurs with partial meniscectomy.

A further limitation of this study was the fact that it was carried out *in vitro*, using a culture media containing fetal bovine serum. This medium was chosen over a chemically defined medium to more closely mimic the complexity of soluble factors present in the *in vivo* environment. Notably, a thicker cellular capsule was observed around these scaffolds, and less collagen/proteoglycan deposition, compared to our previous work employing a prochondrogenic, chemically defined media.[7,8] This capsule slightly confounds the biochemical analysis, as we were unable to remove it before digestion, and may additionally contribute to mechanical integration. Further, we included TGF-β3 to the media to stimulate matrix production and a chondrogenic phenotype; without this growth factor, limited matrix is deposited (*data not shown*). *In vivo*, local delivery of TGF-β3 could be accomplished through entrapped drug-delivering microspheres[39] or other delivery techniques from electropun fibers,[2] to promote matrix deposition.

While many of the cell-based meniscus repair studies noted above employed mesenchymal stem cells, we chose here to focus on MFCs, derived either from the native tissue directly via migration into the scaffold or through isolation and *in vitro* expansion. This choice was made based on the recent observation of phenotypic instability in stem cells with implantation (i.e., a propensity to transition toward hypertrophy and mineralization[40]), as well as the clinical applicability of meniscus cells. For example, we have previously demonstrated that human meniscus cells derived from surgical debris and seeded onto aligned nanofibrous scaffolds deposit a functional, load-bearing extracellular matrix with *in vitro* culture.[41] Despite this, culture-expanded cells are likely phenotypically distinct from the native meniscus cells due to changes during monolayer expansion.[42] Thus, it is unclear if the growth differences seen between tissue-free control scaffolds and scaffold–meniscus constructs are due to changes in cells themselves with passaging, or to the presence of the native tissue. Similarly, meniscus cells for preseeding or preculture were derived from all portions of the meniscus and combined; a more detailed analysis should be conducted using region-specific cell populations. The tissue extracellular matrix is also a depot for growth factors and release of these molecules to the culture system may alter cell behavior.[43] Alternatively, cells within the meniscus tissue may produce factors and signal to the adjacent scaffold,[44] altering its maturation directly. Finally, we used meniscus tissue derived from young (0–3 month) bovine donors; this tissue is hypercellular and has a distinct matrix composition compared to the adult tissue.[18] As meniscus tears occur primarily in the adult human population, additional studies will be required to determine if age-related differences directly impact scaffold maturation and integration capacity.

Conclusions

In this work, we evaluated the impact of nanofiber alignment, scaffold porosity, and cell preseeding on nanofibrous scaffold maturation and integration in an *in vitro* meniscus defect model. This model allows for direct comparison between different scaffold formulations, the best of which can be tested further in more physiologically relevant *in vivo* models. With this work, we identified scaffold attributes that may further our efforts to replace resected meniscus in a manner that promotes regeneration and reestablishes joint mechanics. In particular, the use of highly porous scaffolds, with or without preseeding, resulted in the highest level of scaffold maturation and integration with the native tissue. While an acellular scaffold would represent an off-the-shelf and less expensive device for use in any patient, a cellular or precultured scaffold may significantly reduce repair time; the choice between these different approaches will need to be evaluated in large animal models testing efficacy of integration and maturation. Application of these scaffolds for meniscus repair may 1 day limit the development of cartilage erosion after meniscectomy, forestalling the onset of osteoarthritis and the need for total knee arthroplasty.

Acknowledgments

Funding was provided, in part, by the National Institutes of Health (AR056624) and the Veterans' Administration. We would like to thank Dr. Isaac Erickson for fabrication of the mechanical testing fixture for these studies.

Disclosure Statement

The authors have no competing financial interests to disclose.

References

1. Mauck, R.L., Baker, B.M., Nerurkar, N.L., Burdick, J.A., Li, W.J., Tuan, R.S., *et al.* Engineering on the straight and narrow: the mechanics of nanofibrous assemblies for fiber-reinforced tissue regeneration. Tissue Eng Part B Rev **15,** 171, 2009.
2. Baker, B.M., Handorf, A.M., Ionescu, L.C., Li, W.J., and Mauck, R.L. New directions in nanofibrous scaffolds for soft tissue engineering and regeneration. Expert Rev Med Devices **6,** 515, 2009.

3. Zhong, S.P., Zhang, Y.Z., and Lim, C.T. Tissue scaffolds for skin wound healing and dermal reconstruction. Wiley Interdiscip Rev Nanomed Nanobiotechnol **2,** 510, 2010.
4. Xie, J., MacEwan, M.R., Schwartz, A.G., and Xia, Y. Electrospun nanofibers for neural tissue engineering. Nanoscale **2,** 35, 2010.
5. Sell, S.A., McClure, M.J., Garg, K., Wolfe, P.S., and Bowlin, G.L. Electrospinning of collagen/biopolymers for regenerative medicine and cardiovascular tissue engineering. Adv Drug Deliv Rev **61,** 1007, 2009.
6. Jang, J.H., Castano, O., and Kim, H.W. Electrospun materials as potential platforms for bone tissue engineering. Adv Drug Deliv Rev **61,** 1065, 2009.
7. Baker, B.M., and Mauck, R.L. The effect of nanofiber alignment on the maturation of engineered meniscus constructs. Biomaterials **28,** 1967, 2007.
8. Nerurkar, N.L., Baker, B.M., Sen, S., Wible, E.E., Elliott, D.M., and Mauck, R.L. Nanofibrous biologic laminates replicate the form and function of the annulus fibrosus. Nat Mater **8,** 986, 2009.
9. Baker, B.M., Gee, A.O., Sheth, N.P., Huffman, G.R., Sennett, B.J., Schaer, T.P., *et al.* Meniscus tissue engineering on the nanoscale: from basic principles to clinical application. J Knee Surg **22,** 45, 2009.
10. Pittenger, M.F., Mackay, A.M., Beck, S.C., Jaiswal, R.K., Douglas, R., Mosca, J.D., *et al.* Multilineage potential of adult human mesenchymal stem cells. Science **284,** 143, 1999.
11. Baker, B.M., Nathan, A.S., Gee, A.O., and Mauck, R.L. The influence of an aligned nanofibrous topography on human mesenchymal stem cell fibrochondrogenesis. Biomaterials **31,** 6190, 2010.
12. Mandal, B.B., Park, S.-H., Gil, E.S., and Kaplan, D.L. Multilayered silk scaffolds for meniscus tissue engineering. Biomaterials **32,** 639, 2011.
13. Warnock, J.J., Fox, D.B., Stoker, A.M., and Cook, J.L. Evaluation of *in vitro* growth factor treatments on fibrochondrogenesis by synovial membrane cells from osteoarthritic and nonosteoarthritic joints of dogs. Am J Vet Res **72,** 500, 2011.
14. Nerurkar, N.L., Sen, S., Baker, B.M., Elliott, D.M., and Mauck, R.L. Dynamic culture enhances stem cell infiltration and modulates extracellular matrix production on aligned electrospun nanofibrous scaffolds. Acta Biomater **7,** 485, 2011.
15. Baker, B.M., Gee, A.O., Metter, R.B., Nathan, A.S., Marklein, R.A., Burdick, J.A., *et al.* The potential to improve cell infiltration in composite fiber-aligned electrospun scaffolds by the selective removal of sacrificial fibers. Biomaterials **29,** 2348, 2008.
16. Baker, B.M., Nerurkar, N.L., Burdick, J.A., Elliott, D.M., and Mauck, R.L. Fabrication and modeling of dynamic multipolymer nanofibrous scaffolds. J Biomech Eng **131,** 101, 2009.
17. Arendt, E.A. Orthopaedic Knowledge Update: Sports Medicine 2. Rosemont, IL: American Academy of Orthopaedic Surgeons, 1999.
18. Ionescu, L.C., Lee, G.C., Garcia, G.H., Zachry, T.L., Shah, R.P., Sennett, B.J., *et al.* Maturation state-dependent alterations in meniscus integration: implications for scaffold design and tissue engineering. Tissue Eng Part A **14,** 193, 2011.
19. McNulty, A.L., Moutos, F.T., Weinberg, J.B., and Guilak, F. Enhanced integrative repair of the porcine meniscus *in vitro* by inhibition of interleukin-1 or tumor necrosis factor alpha. Arthritis Rheum **6,** 3033, 2007.
20. McNulty, A.L., and Guilak, F. Integrative repair of the meniscus: lessons from *in vitro* studies. Biorheology **45,** 487, 2008.
21. van de Breevaart Bravenboer, J., In der Maur, C.D., Bos, P.K., Feenstra, L., Verhaar, J.A., Weinans, H., *et al.* Improved cartilage integration and interfacial strength after enzymatic treatment in a cartilage transplantation model. Arthritis Res Ther **6,** R469, 2004.
22. McNulty, A.L., Weinberg, J.B., and Guilak, F. Inhibition of matrix metalloproteinases enhances *in vitro* repair of the meniscus. Clin Orthop Relat Res **467,** 1557, 2009.
23. Rodkey, W.G., DeHaven, K.E., Montgomery, W.H., Baker, C.L.J., Beck, C.L.J., Hormel, S.E., *et al.* Comparison of the collagen meniscus implant with partial meniscectomy. A prospective randomized trial. J Bone Joint Surg Am **90,** 1413, 2008.
24. Nerurkar, N.L., Han, W., Mauck, R.L., and Elliott, D.M. Homologous structureâ€"function relationships between native fibrocartilage and tissue engineered from MSC-seeded nanofibrous scaffolds. Biomaterials **32,** 461, 2010.
25. Farndale, R.W., Buttle, D.J., and Barrett, A.J. Improved quantitation and discrimination of sulphated glycosaminoglycans by use of dimethylmethylene blue. Biochim Biophys Acta **883,** 173, 1986.
26. Nam, J., Huang, Y., Agarwal, S., and Lannutti, J. Improved cellular infiltration in electrospun fiber via engineered porosity. Tissue Eng **13,** 2249, 2007.
27. Pham, Q.P., Sharma, U., and Mikos, A.G. Electrospun poly(epsilon-caprolactone) microfiber and multilayer nanofiber/microfiber scaffolds: characterization of scaffolds and measurement of cellular infiltration. Biomacromolecules **7,** 2796, 2006.
28. Gupta, P., and Wilkes, G.L. Some investigations on the fiber formation by utilizing a side-by-side bicomponent electrospinning approach. Polymer **44,** 6353, 2003.
29. Newman, A.P., Anderson, D.R., Daniels, A.U., and Dales, M.C. Mechanics of the healed meniscus in a canine model. Am J Sports Med **17,** 164, 1989.
30. Scholten, P.M., Ng, K.W.J., K., Serino, L.P., Warren, R.F., Torzilli, P.A., and Maher, S.A. A semi-degradable composite scaffold for articular cartilage defects. J Biomed Mater Res A **97A,** 8, 2011.
31. Pabbruwe, M.B., Kafienah, W., Tarlton, J.F., Mistry, S., Fox, D.J., and Hollander, A.P. Repair of meniscal cartilage white zone tears using a stem cell/collagen-scaffold implant. Biomaterials **31,** 2583, 2009.
32. van Tienen, T.G., Heijkants, R.G., Buma, P., de Groot, J.H., Pennings, A.J., and Veth, R.P. Tissue ingrowth and degradation of two biodegradable porous polymers with different porosities and pore sizes. Biomaterials **23,** 1731, 2002.
33. Heijkants, R.G., van Calck, R.V., De Groot, J.H., Pennings, A.J., Schouten, A.J., van Tienen, T.G., *et al.* Design, synthesis and properties of a degradable polyurethane scaffold for meniscus regeneration. J Mater Sci Mater Med **15,** 423, 2004.
34. Peretti, G.M., Gill, T.J., Xu, J.W., Randolph, M.A., Morse, K.R., and Zaleske, D.J. Cell-based therapy for meniscal repair: a large animal study. Am J Sports Med **32,** 146, 2004.
35. Angele, P., Johnstone, B., Kujat, R., Zellner, J., Nerlich, M., Goldberg, V., *et al.* Stem cell based tissue engineering for meniscus repair. J Biomed Mater Res A **85,** 445, 2008.
36. Hennerbichler, A., Moutos, F.T., Hennerbichler, D., Weinberg, J.B., and Guilak, F. Repair response of the inner and

outer regions of the porcine meniscus *in vitro*. Am J Sports Med **35,** 754, 2007.
37. Webber, R.J., York, J.L., Vanderschilden, J.L., and Hough, A.J.J. An organ culture model for assaying wound repair of the fibrocartilaginous knee joint meniscus. Am J Sports Med **17,** 393, 1989.
38. Schenker, M.L., Huang, K.L., Bonilla, A., Fisher, M.B., Shah, R.P., Ionescu, L.C., *et al.* Dynamic Nanofibrous Scaffolds Improve In Vivo Colonization and Implant Fixation in a Meniscus Defect Model. Orthopedic Research Society Annual Conference, San Francisco, 2011.
39. Ionescu, L.C., Lee, G.C., Sennett, B.J., Burdick, J.A., and Mauck, R.L. An Anisotropic Nanofiber/Microsphere Composite with Controlled Release of Biomolecules For Fibrous Tissue Engineering. Biomaterials **31,** 4113, 2010.
40. Pelttari, K., Winter, A., Steck, E., Goetzke, K., Hennig, T., Ochs, B.G., *et al.* Premature induction of hypertrophy during *in vitro* chondrogenesis of human mesenchymal stem cells correlates with calcification and vascular invasion after ectopic transplantation in SCID mice. Arthritis Rheum **54,** 3254, 2006.
41. Baker, B.M., Nathan, A.S., Huffman, G.R., and Mauck, R.L. Tissue engineering with meniscus cells derived from surgical debris. Osteoarthr Cartilage **17,** 336, 2009.
42. Gunja, N.J., and Athanasiou, K.A. Passage and reversal effects on gene expression of bovine meniscal fibrochondrocytes. Arthritis Res Ther **9,** R93, 2007.
43. Gentili, C., and Cancedda, R. Cartilage and bone extracellular matrix. Curr Pharm Des **15,** 1334, 2009.
44. Tan, A.R., Dong, E.Y., Andry, J.P., Bulinski, J.C., Ateshian, G.A., and Hung, C.T. Coculture of engineered cartilage with primary chondrocytes induces expedited growth. Clin Orthop Relat Res **469,** 2735, 2011.

Address correspondence to:
Robert L. Mauck, PhD
McKay Orthopaedic Research Laboratory
Department of Orthopaedic Surgery
Perelman School of Medicine
University of Pennsylvania
36th Street and Hamilton Walk
Philadelphia, PA 19104

E-mail: lemauck@mail.med.upenn.edu

Received: January 29, 2012
Accepted: September 19, 2012
Online Publication Date: December 3, 2012